# Electronic Supplementary Information

# Enhanced performance of ternary organic solar cells with a wide bandgap acceptor as third component

He Huang[a,b], Xiaojun Li[a,b*], Shanshan Chen[c,d], Beibei Qiu[a,b], Jiaqi Du[a,b], Lei Meng[b,*], Zhanjun Zhang[a,*], Changduk Yang[c], Yongfang Li[a,b,e*]

[a]School of Chemical Science, University of Chinese Academy of Sciences, Beijing 100049, China

[b]CAS Research/Education Center for Excellence in Molecular Sciences, CAS Key Laboratory of Organic Solids, Institute of Chemistry, Chinese Academy of Sciences, Beijing 100190, China

[c]Department of Energy Engineering, School of Energy and Chemical Engineering, Low Dimensional Carbon Materials Center, Ulsan National Institute of Science and Technology (UNIST), Ulsan 689-798, South Korea

[d]MOE Key Laboratory of Low-grade Energy Utilization Technologies and Systems, CQU-NUS Renewable Energy Materials & Devices Joint Laboratory, School of Energy & Power Engineering, Chongqing University, Chongqing 400044, China.

[e]Laboratory of Advanced Optoelectronic Materials, College of Chemistry, Chemical Engineering and Materials Science, Soochow University, Suzhou, Jiangsu 215123, China

Email: lixiaojun@iccas.ac.cn; menglei@iccas.ac.cn; zhangzj@ucas.ac.cn; liyf@iccas.ac.cn;

## Experimental Section

### Materials

Unless otherwise stated, all the solvents and chemicals were obtained commercially

and were used without further purification.

**Synthesis of C8-SF**

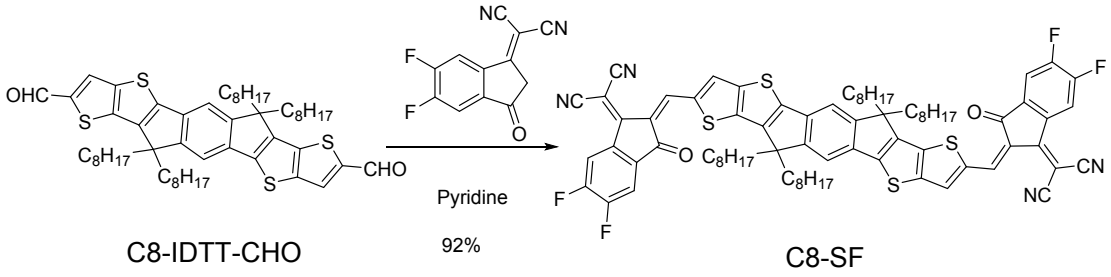


C8-IDTT-CHO C8-SF

Compound C8-IDTT-CHO (176 mg, 0.2 mmol) and 2-(5 and 6-difluoro-3-oxo-2,3-dihydro-1H-inden-1-ylidene) malononitrile (300 mg, 1.4 mmol) were dissolved in $CHCl_3$ (25 mL) under a nitrogen atmosphere. 0.6 ml pyridine was added and refluxed for 12 h. Then, the mixture was poured into water (100 mL) and extracted with $CHCl_3$ (2 × 100 mL). The organic layer was washed with water, and then dried over $MgSO_4$. After removing the solvent, the residue was purified using column chromatography on silica gel employing petroleum ether/$CHCl_3$ (1:4) as an eluent, yielding a dark blue solid C8-SF (240 mg, 92%). $^1$H NMR (300 MHz, $CDCl_3$) δ 8.98 (s, 2H), 8.56 (dd, J = 9.8, 6.5 Hz, 2H), 8.24 (s, 2H), 7.72 (t, J = 7.5 Hz, 2H), 7.50 (s, 2H), 2.42 – 1.98 (m, 8H), 1.07 (s, 40H), 0.76 (m, 20H). $^{13}$C NMR (75 MHz, $CDCl_3$) δ 186.05, 158.29, 156.34, 155.06, 154.73, 147.72, 147.33, 143.87, 138.99, 138.62, 138.06, 137.93, 136.77, 136.73, 136.66, 136.63, 134.55, 134.52, 134.47, 134.44, 121.34, 115.18, 114.94, 114.30, 114.25, 112.76, 112.51, 77.44, 69.71, 54.80, 38.24, 31.74, 29.69, 29.17, 29.09, 24.14, 22.57, 14.05. HRMS (TOF) m/z calcd for $[M]^+$ $C_{78}H_{78}F_4N_4O_2S_4$ 1306.4944, found 1306.4953.

**Synthesis of Y-MODF**

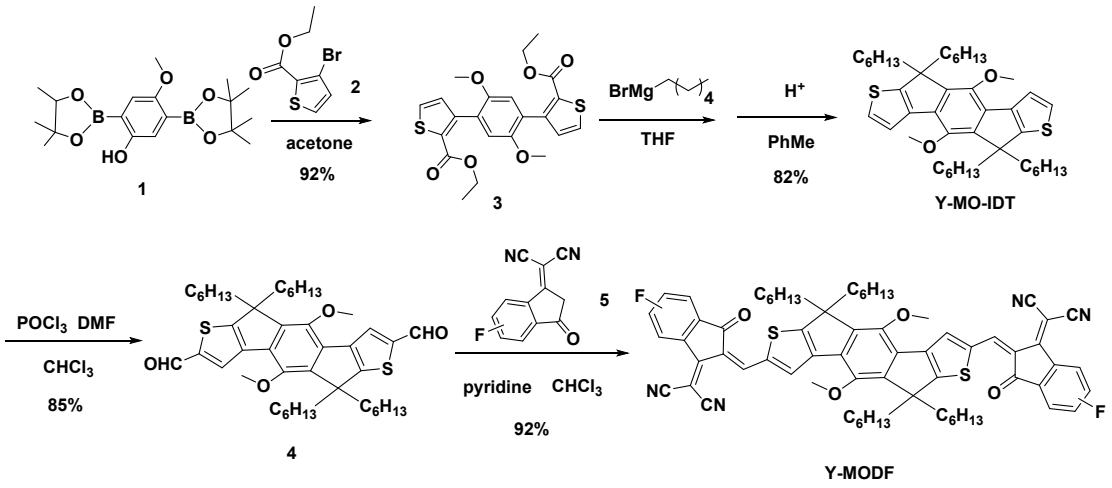


Compound **1, 2** were synthesized according to the method in the literature1. Intermediate **3** was prepared from the reaction of **1** and **2** by Suzuki reaction using $Pd(OAc)_2$ and tri-tert-butylphosphine tetrafluoroborate as catalyst at room temperature. The crude product **3** was purified directly by washing with petroleum ether. Then Compound **3** was dissolved in THF and reacted with hexylmagnesium bromide to give intermediate Y-MO-IDT. Intermediate **4** was prepared by Vilsmeie-Haack reaction of Y-MO-IDT with $POCl_3$ and DMF. Subsequent Knoevenagel condensation between **4** and compound **5** afforded Y-MODF in high yields.

**Synthesis of Compound 3**

Compound **1** (1.95 g, 5 mmol), Compound **2** (2.56 g, 11 mmol), $Pd(OAc)_2$ (56 mg, 0.25 mmol) and $tBu_3PHBF_4$ (144 mg, 0.5 mmol) were dissolved in acetone (60 mL) under a nitrogen atmosphere. After stirred for 5 min, 8 mL NaOH aqueous solution (2M) was added, and the reaction mixture was stirred for 1 h, then the mixture was extracted with dichloromethane (100 mL × 3) and water (100 mL). The collected organic layer was dried over $MgSO_4$. After removal of the solvent under reduced pressure, the residue was purified by washing with methanol and petroleum ether to give a white product **3** (1.75 g, 91% yield). $^1$H NMR (400 MHz, $CDCl_3$) δ 7.51 (d, J = 5.0 Hz, 2H), 7.12 (d, J = 5.0 Hz, 2H), 6.87 (s, 2H), 4.23 (q, J = 7.1 Hz, 4H), 3.70 (s, 6H), 1.23 (t, J = 7.1 Hz, 6H). $^{13}$C NMR (101 MHz, $CDCl_3$) δ 162.19, 150.31, 143.56, 131.68, 129.42, 129.33, 125.52, 113.97, 60.80, 56.25, 14.11. MS (EI+) m/z calcd for $[M]^+$ $C_{22}H_{22}O_6S_2$ 446, found 446.

**Synthesis of Compound Y-MO-IDT**

Compound **3** (1.93 g 5 mmol) was dissolved in dry THF (60 mL) and placed under a nitrogen atmosphere. The solution was cooled to 0 °C and stirred while 32 mL hexylmagnesium bromide (0.8 M) was added dropwise. The mixture was warmed to room temperature and stirred for 12 h. It was then poured into water and extracted with dichloromethane. The organic extracts were dried over anhydrous $MgSO_4$. After removal of the solvent, the residue was dissolved in dry toluene (30 mL) and placed under a nitrogen atmosphere, then amberlyst15 (2 g) as catalyst (Acros Amberlyst15, (dry) ion-exchange resin) was added and heated at 85 °C for 12 h. After the reaction, the mixture was filtered and the organic liquids were collected. The catalyst was washed with dichloromethane for recycle After removal of the solvent under reduced pressure, the residue was purified by column chromatography on silica gel using petroleum ether as eluent to give white solid. Y-MO-IDT (1.83 g, 92% yield). $^1$H NMR (300 MHz, $CDCl_3$) δ 7.62 (d, J = 4.8 Hz, 2H), 7.05 (d, J = 4.8 Hz, 2H), 3.91 (s, 6H), 2.26-1.97 (m, 8H), 1.12-1.06 (m, 24H), 0.80-0.72 (m, 20H). $^{13}$C NMR (75 MHz, $CDCl_3$) δ 152.64, 143.69, 143.16, 135.55, 128.86, 125.29, 118.92, 59.14, 53.36, 36.02, 29.64, 27.58, 22.22, 20.52, 11.95. HRMS (TOF) m/z calcd for $[M]^+$ $C_{42}H_{62}O_2S_2$ 662.4182, found 662.4185.

**Synthesis of Compound 4**

A Vilsmeier reagent, which was prepared with $POCl_3$ (0.62 mL, 6.4 mmol) in DMF (2.00 mL, 25.84 mmol), was added to a cold solution of Compound Y-MO-IDT (212 mg, 0.32 mmol) in dry $CHCl_3$ (20 mL) at 0 °C under a nitrogen atmosphere. After being stirred at 60 °C for 12 h, the mixture was poured into ice water (100 mL), neutralized with $Na_2CO_3$, and then extracted with dichloromethane. The combined organic layer was washed with water and brine, dried over anhydrous $MgSO_4$. After removal of solvent, it was purified by column chromatography on silica gel using petroleum ether/dichloromethane (1:1) as eluent, yielding a yellow solid 4 (196 mg, 85% yield). $^1$H NMR (400 MHz, $CDCl_3$) δ 9.96 (s, 2H), 7.94 (s, 2H), 3.94 (s, 6H), 2.31-2.04 (m, 8H), 1.14-1.10 (m, 24H), 0.78-0.75 (m, 20H). $^{13}$C NMR (101 MHz, $CDCl_3$) δ 182.92, 163.86, 147.27, 146.71, 145.31, 142.64, 130.10, 129.46, 61.28,

57.69, 39.07, 31.55, 29.71, 29.38, 24.16, 22.50, 13.95. HRMS (TOF) m/z calcd for $[M]^+$ $C_{44}H_{62}O_4S_2$ 718.4090, found 718.4084.

**Synthesis of Compound Y-MODF**

Compound **4** (145 mg, 0.2 mmol) and 2-(5 or 6-difluoro-3-oxo-2,3-dihydro-1H-inden-1-ylidene) malononitrile (300 mg, 1.4 mmol) were dissolved in $CHCl_3$ (25 mL) under a nitrogen atmosphere. 0.6 ml pyridine was added and refluxed for 12 h. Then, the mixture was poured into water (100 mL) and extracted with $CHCl_3$ (2 × 100 mL). The organic layer was washed with water, and then dried over $MgSO_4$. After removing the solvent, the residue was purified using column chromatography on silica gel employing petroleum ether/$CHCl_3$ (1:4) as an eluent, yielding a dark blue solid Y-MODF (203 mg, 92%). $^1$H NMR (300 MHz, $CDCl_3$) δ 9.00 (s, 2H), 8.75 (m, 1H), 8.41 (d, J = 8.6 Hz, 2H), 8.12 (m, 2H), 7.97 (dd, J = 8.4, 5.2 Hz, 1H), 7.59 (d, J = 5.8 Hz, 1H), 7.44 (m, 2H), 3.99 (s, 6H), 2.50 – 2.08 (m, 8H), 1.31 – 1.00 (m, 24H), 0.96 – 0.67 (m, 20H). $^{13}$C NMR (75 MHz, $CDCl_3$) δ 195.56, 186.82, 174.76, 174.59, 168.49, 165.07, 159.67, 159.40, 147.11, 146.05, 145.39, 143.86, 142.30, 142.16, 141.36, 141.30, 140.16, 140.08, 140.04, 138.86, 138.74, 136.56, 135.83, 133.26, 130.13, 128.03, 127.91, 126.12, 125.98, 122.62, 122.42, 122.32, 122.24, 121.93, 114.55, 114.33, 114.16, 114.07, 113.05, 112.70, 111.01, 110.70, 99.99, 70.68, 61.33, 58.91, 39.59, 31.58, 29.43, 24.43, 22.53, 13.96. HRMS (TOF) m/z calcd for $[M]^+$ $C_{68}H_{68}F_2N_4O_4S_2$ 1106.4650, found 1106.4658.

**Device fabrication and characterization**

The PSCs were fabricated with a structure of ITO/PEDOT: PSS /active layer/cathode. A thin layer of PEDOT: PSS was deposited through spin-coating on pre-cleaned ITO-coated glass at 4500 rpm and dried subsequently at 150 ℃ for 15 min. Then the device was transferred to a nitrogen glove box, and the active blend layer of PM6:C8-SF, PM6:Y-MODF and PM6:C8-S:Y-MODF were spin-coated onto the PEDOT: PSS layer. Then the devices were annealed at 130 ℃ for 5 min to improve the morphology of the active layers. After that, PDINO in methanol solution with a concentration of 1.0 mg $mL^{-1}$ was deposited to act as intermediate layer of cathode with a thickness of

ca. 15 nm. Finally, top Al electrode was deposited in vacuum onto the cathode buffer layer at a pressure of $1.0\times 10^{-4}$ Pa. The active area of the device was 4.6 mm2. The current density–voltage(J–V) characteristics of the OSCs were measured on a computer-controlled Keithley 2450 Source-Measure Unit. Oriel Sol3A Class AAA Solar Simulator (model, Newport 94023A) with a 450 W xenon lamp and an air mass (AM) 1.5 filter was used as the light source. The External Quantum Efficiency (EQE) spectra were measured by Solar Cell Spectral Response Measurement System QE-R3-011 (Enli Technology Co., Ltd., Taiwan). The light intensity at each wavelength was calibrated with a standard single-crystal Si photovoltaic cell. The UV–vis absorption spectra of solution and film were measured on a Hitachi U-3010 UV–vis spectrophotometer and the PL spectra were measured with a Shimadzu RF-5301PC fluorescence spectrophotometer. The film morphology were measured using an AFM (SPA-400) and TEM (Libra 200). GIWAXS measurements were carried out using small angle X-ray scattering system.

**Mobility measurements**

The mobility are measured with the device structure of ITO/PEDOT:PSS/active layer/$MoO_3$/Ag for hole-mobility and ITO/ZnO/active layer/PDINO/Al for electron-mobility. The hole and electron mobilities are calculated according to the space charge limited current (SCLC) method equation: $J = 9\mu\varepsilon^r\varepsilon^0V^2/8L^3$, where J is the current density, μ is the hole or electron mobility,$\varepsilon^0$ is the permittivity of empty space, $\varepsilon^r$ is the relative dielectric constant of active layer material, V is the internal voltage in the device, and L is the thickness of the active layer.

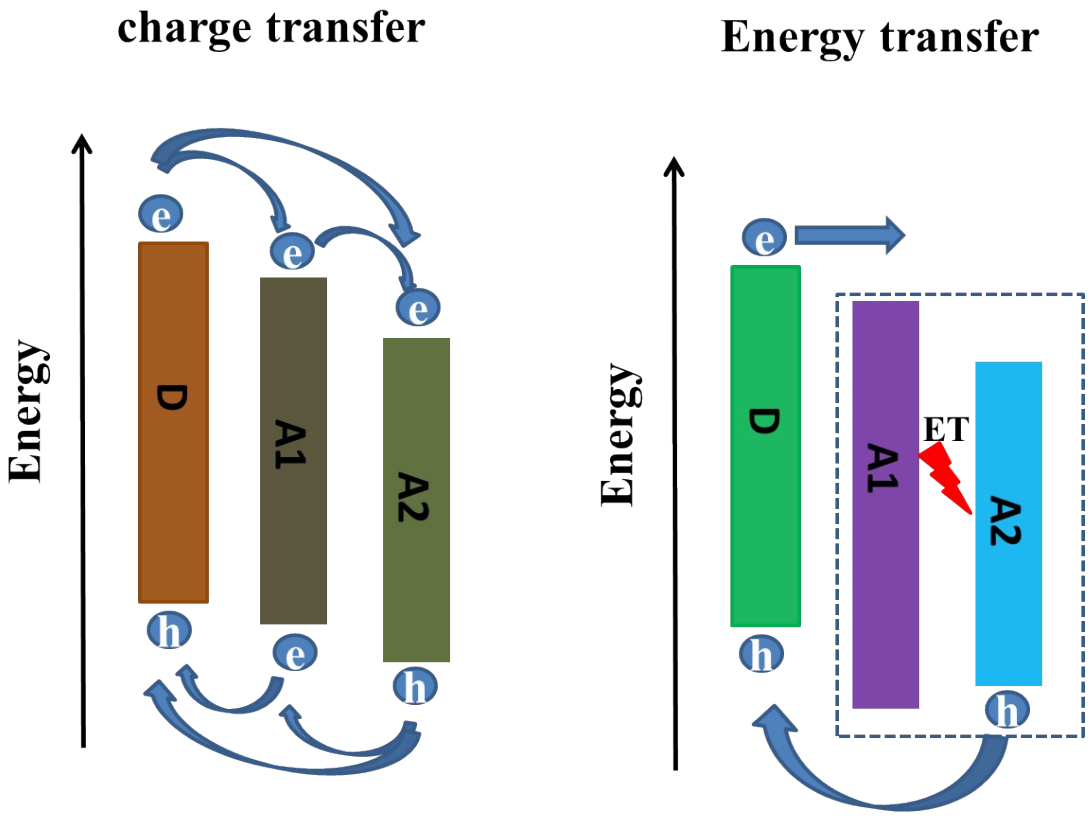


**Figure S1**. Schematic of the electron transfer and energy transfer in multiple-acceptor system.

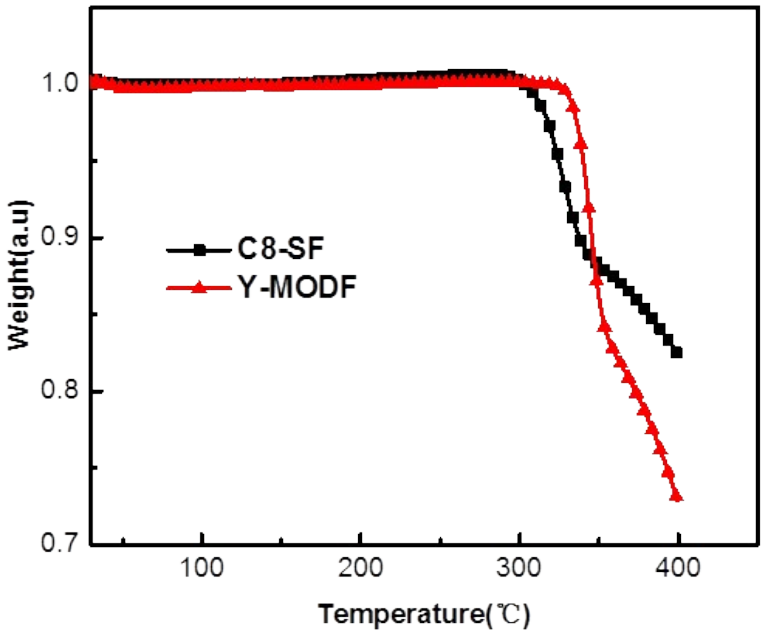


**Figure S2**. The TGA plot of C8-SF and Y-MODF.

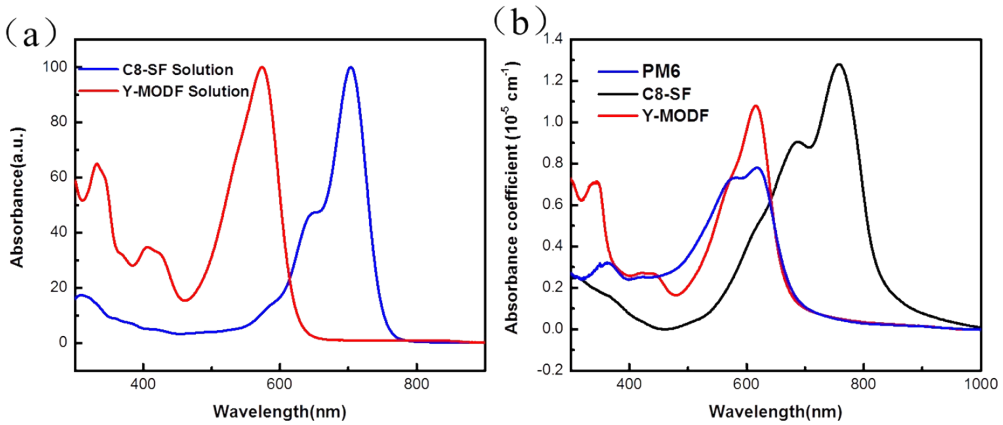


**Figure S3**. a) The solution absorption of pure acceptor and b) the absorption coefficient of donor and acceptor film.

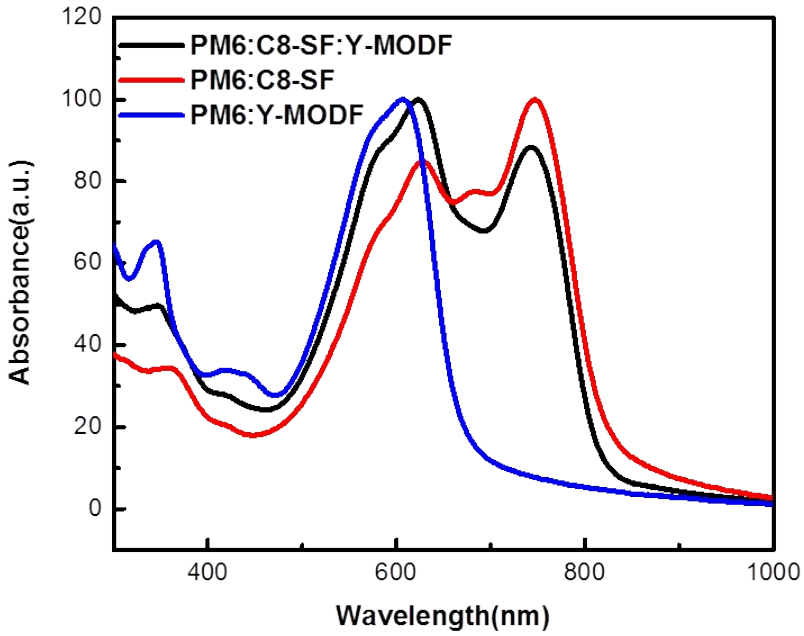


**Figure S4**. The absorption of the blend film.

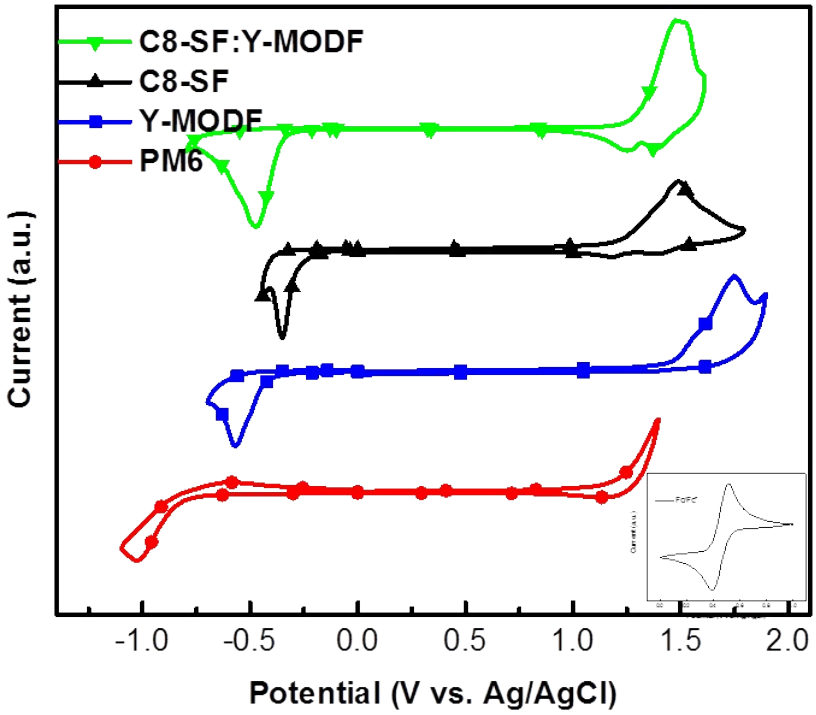


**Figure S5**. The electrochemical cyclic voltammograms of the pristine donor and acceptor film and the C8-SF:Y-MODF((w:w 3:1) blend film.

**Table S1**. Electronic Energy Levels and Optical Properties of PM6, C8-SF and Y-MODF and the C8-SF:Y-MODF((w:w 3:1) blend film.

| | $\lambda_{max}$[a] [nm] | $\lambda_{edge}$[a] [nm] | $E_g^{opt}$[b] [eV] | $E_{HOMO}$[c] [eV] | $E_{LUMO}$[c] [eV] |
|---|---|---|---|---|---|
| PM6 | 615 | 675 | 1.84 | -5.49 | -3.60 |
| Y-MODF | 616 | 667 | 1.86 | -5.81 | -3.90 |
| C8-SF | 759 | 822 | 1.51 | -5.53 | -4.05 |
| C8-SF:Y-MODF | | | | -5.60 | -4.00 |

[a]Absorption of the films; [b]Calculated from the absorption edge of the molecule films: $E_g^{opt} = 1240/\lambda_{edge}$; [c]Calculated according to the equation $E_{LUMO/HOMO} = -e\ (\varphi_{red/ox} +$

4.34) [eV].

**Table S2**. The photovoltaic performance of as-cast OSCs with different donor/acceptor weight ratios.

| **PM6:C8-SF:Y-MODF（as cast）** | $V_{oc}$ **(V)** | $J_{sc}(J_{cal})$ **(mA cm$^{-2}$)** | **FF (%)** | **PCE(%)** |
|---|---|---|---|---|
| 1:1.2:0 | 0.825 | 18.72(18.52) | 73.22 | 11.37 |
| 1:1.1:0.1 | 0.856 | 19.68(19.38) | 73.49 | 12.38 |
| 1:1.0:0.2 | 0.863 | 19.99(19.77) | 74.12 | 12.76 |
| 1:0.9:0.3 | 0.876 | 20.02(19.17) | 73.83 | 12.95 |
| 1:0.8:0.4 | 0.895 | 19.31(18.80) | 73.01 | 12.62 |
| 1:0.7:0.5 | 0.922 | 18.79(18.26) | 69.33 | 12.01 |
| 1:0.5:0.7 | 0.915 | 18.00(17.78) | 63.23 | 10.41 |
| 1:0:1.2 | 0.994 | 11.86(11.83) | 54.17 | 6.38 |

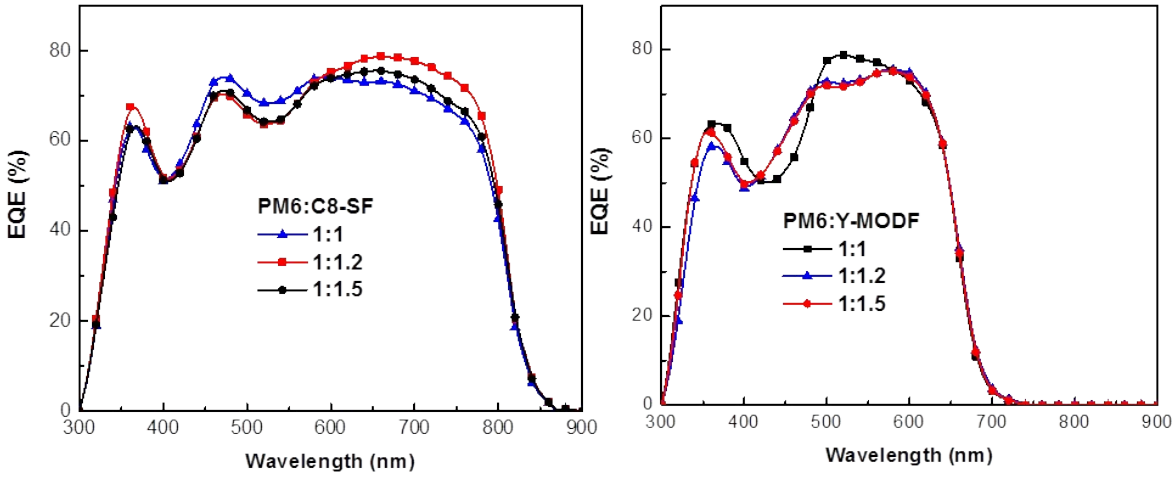


**Figure S6**. The EQE spectra of the binary OSCs with different D/A weight ratios.

**Table S3**. The photovoltaic performance of the binary OSCs with different D/A weight ratios.

| **PM6:C8-SF** | $V_{oc}$ **(V)** | $J_{sc}(J_{cal})$ **(mA cm$^{-2}$)** | **FF (%)** | **PCE (%)** |
|---|---|---|---|---|
| 1:1 | 0.790 | 19.78(19.16) | 72.00 | 11.25 |
| 1:1.2 | 0.787 | 20.03(19.78) | 73.15 | 11.53 |
| 1:1.5 | 0.787 | 19.64(19.19) | 73.53 | 11.36 |
| **PM6:Y-MODF** | | | | |
| 1:1 | 0.983 | 12.36(12.01) | 71.84 | 8.73 |
| 1:1.2 | 0.984 | 12.30(12.04) | 71.55 | 8.63 |
| 1:1.5 | 0.981 | 12.38(11.96) | 71.91 | 8.73 |

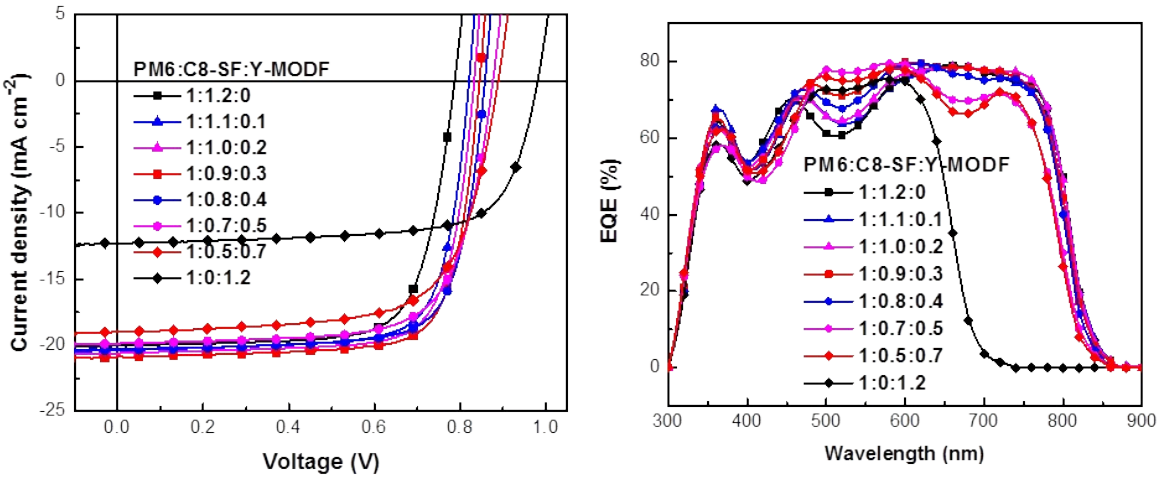


**Figure S7**. The *J-V* curves and EQE spectra of the ternary OSCs based on PM6:C8-SF:Y-MODF with different weight ratios.

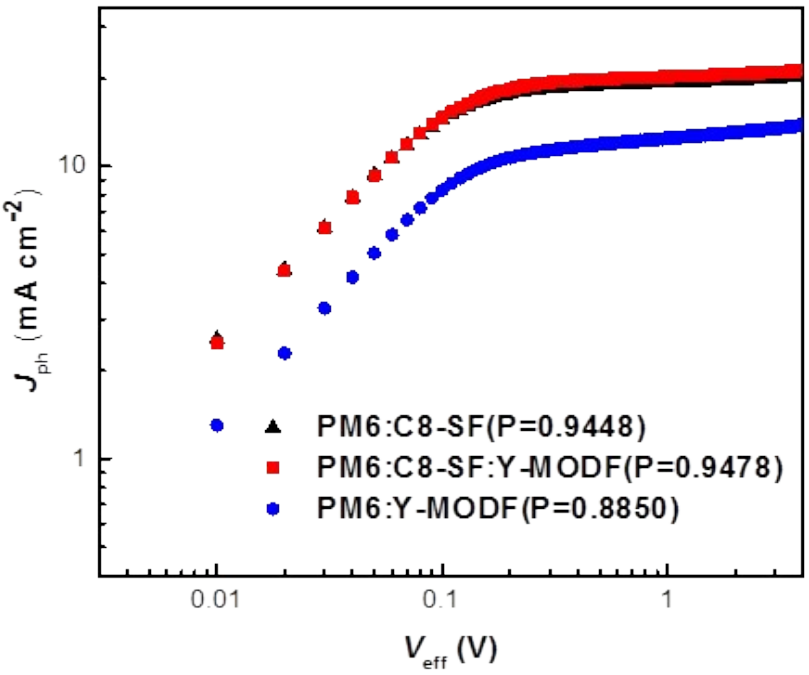


**Figure S8**. The plots of photocurrent density ($J_{ph}$) *versus* effective voltage ($V_{eff}$) of the binary and optimal ternary OSCs.

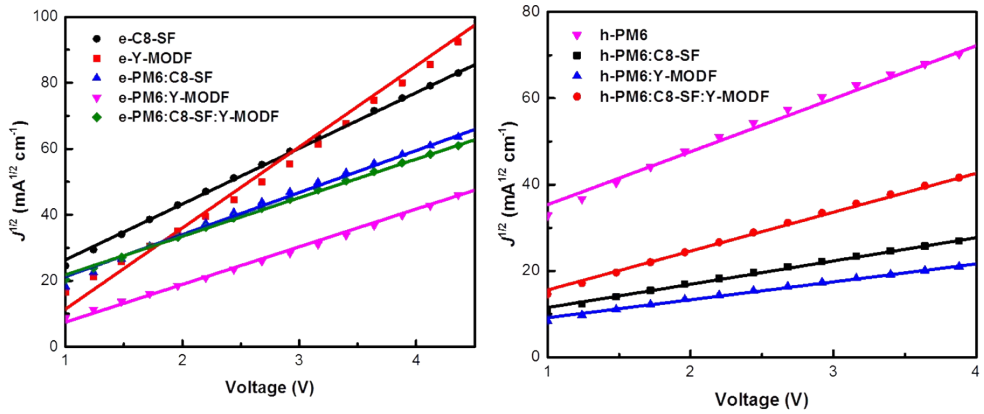


**Figure S9**. The charge mobilities measurement plots of pure materials and blend films with thermal annealing at 130°C for 5 minutes.

**Table S4**. The charge mobilities of PM6, C8-SF, Y-MODF pure films and their blend films with thermal annealing at 130°C for 5 minutes.

| | $\mu_e$ (*$10^{-4}$ $cm^2$ $V^{-1}$ $s^{-1}$) | $\mu_h$ (*$10^{-4}$ $cm^2$ $V^{-1}$ $s^{-1}$) | $\mu_e/\mu_h$ |
|---|---|---|---|
| PM6 | | 4.79 | |
| C8-SF | 7.75 | | |
| Y-MODF | 11.16 | | |
| PM6:C8-SF | 9.58 | 5.70 | 1.68 |
| PM6:Y-MODF | 10.51 | 1.95 | 5.37 |
| PM6:C8-SF:Y-MODF | 7.84 | 5.90 | 1.33 |

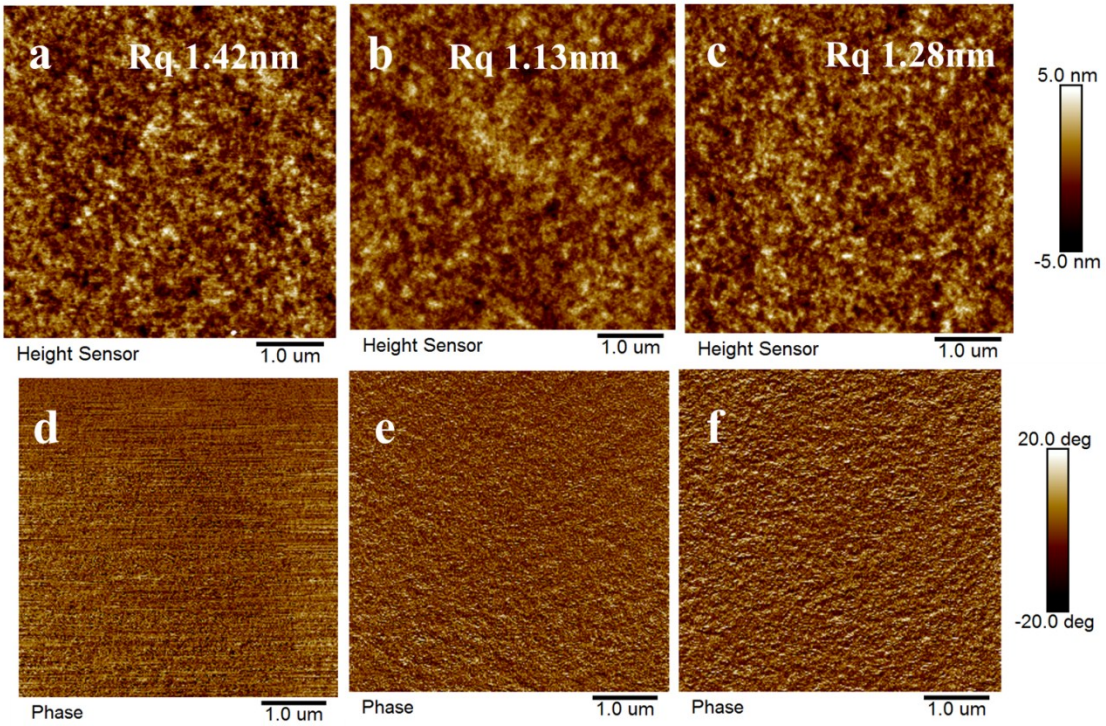


**Figure S10**. The AFM height (upper) and phase (lower) images of a, d) PM6:C8-SF, b, c) PM6:Y-MODF and e, f) optimal PM6:C8-SF:Y-MODF blend film.

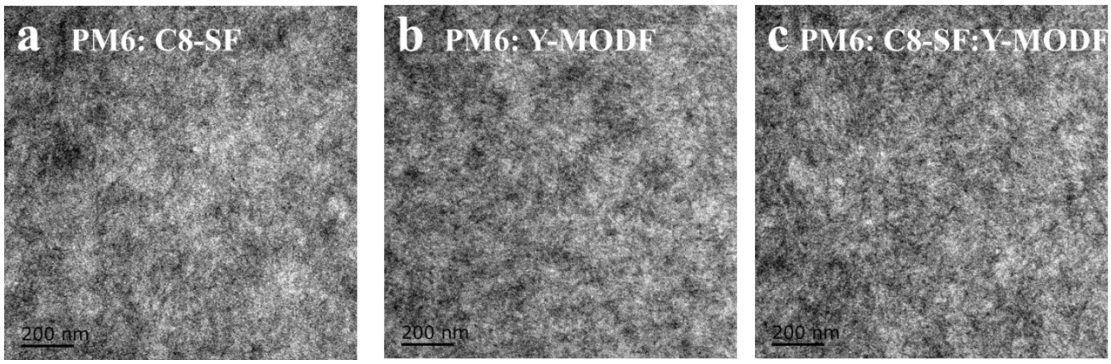


**Figure S11**. The TEM images of binary and optimal ternary active layer.

## Reference

1 X. J. Li, F. Pan, C. K. Sun, M. Zhang, Z. W. Wang, J. Q. Du, J. Wang, M. Xiao, L. W. Xue, Z. G. Zhang, C. F. Zhang, F. Liu and Y. F. Li, *Nat. Commun.*, 2019, **10**. 519.